Strong coupling between two distant electronic spins via a nanomechanical resonator

Li-gong Zhou,[1] L. F. Wei,[2,*] Ming Gao,[1,3] and Xiang-bin Wang[1,†]

[1]*Department of Physics, Tsinghua University, Beijing 100084, People's Republic of China*

[2]*Quantum Optoelectronics Institute, Southwest Jiaotong University, Chengdu 610031, People's Republic of China*

[3]*Department of Physics, National University of Defense Technology, Changsha 410073, People's Republic of China*

(Received 24 January 2010; published 26 April 2010)

We propose a scheme to achieve a strong coupling between two distant symmetrically placed electronic spins (such as nitrogen-vacancy centers in diamonds) by using a quantized nanomechanical resonator (NAMR) as a data bus. These distant spins (without any direct interaction) simultaneously couple to a common NAMR. When the detunings between effective spin transition frequencies and the fundamental frequency of the NAMR are large enough, an effective coupling could be induced between the two distant electronic spins. The value of such a coupling could be significantly large (i.e., up to a few kilohertz). This induced interaction between the two spins can be used to implement an iSWAP quantum gate, and to probabilistically prepare two-spin maximal entangled states by detecting the frequency shifts of the NAMR.

DOI: 10.1103/PhysRevA.81.042323 PACS number(s): 03.67.Bg, 03.67.Lx, 71.55.−i, 76.30.Mi

I. INTRODUCTION

Electronic spins, which can be realized with nitrogen-vacancy (N-*V*) impurities in diamonds [1], are expected to implement quantum information processing (QIP) [2,3] due to their long decoherence time [4]. However, in practice it is not easy to achieve controllable entanglement between these spins with a typical distance of tens of nanometers to maintain their weak magnetic interactions.

With advances in micro-manufacturing technologies, it is possible to produce nanomechanical resonators (NAMRs) with high quality factors, high resonance frequencies, and small effective masses [5–7]. These artificial structures could be utilized for high precision detectors [5,8–12] and to test quantum phenomena at macroscopic scales [13–19]. Specifically, NAMRs provide an attractive platform for detecting and controlling single spins [20–22].

Recently, the coupling between single electronic spins and NAMRs has been extensively investigated. The detection of a single electronic spin by a classical cantilever-type NAMR was reported in Ref. [21]. Later, by quantizing the motion of an NAMR, P. Rabl *et al.* [22] found that it is possible to achieve strong coupling between an NAMR's quantized motion and a spin qubit generated by an N-*V* impurity. The coupling strength can reach about 100 kHz, which considerably exceeds both the spin's decoherence time and the NAMR's intrinsic damping rate. Subsequently, P. Rabl *et al.* [23] proposed a universal realization of a quantum data bus for electronic spins, which were coupled to the motion of magnetized mechanical resonators via the magnetic-field gradients. Furthermore, when the Rabi frequency of the vibration of the driving microwave (applied to the spin qubit) and that of the NAMR were near-resonant, Z. Y. Xu *et al.* [24] showed that the Dicke States of N-*V* centers in a line located in nanoscale diamonds could be prepared.

In this article, we study the coupling between two distant electronic spins (generated by, for example, two N-*V* centers in different diamonds) via a quantum NAMR. Two magnetic tips are attached to the free end of the NAMR on either sides of which there are two symmetrically positioned electronic spins. Microwaves are applied to drive the Rabi oscillations between the states of single spins. The oscillations of the two tips produce a time-varying magnetic field proportional to the NAMR's displacement. By such a magnetic-field gradient, two distant spins simultaneously couple to the NAMR. We show that, if the spins and the NAMR work within the so-called large detuning regime, strong coupling (up to a few kilohertz) between these two distant spins can be achieved. More importantly, this coupling strength can be controlled by adjusting the driving microwave's frequency and the Rabi frequency between the spins' two states. We then show that how this induced interaction between the two distant spins can be used to implement an iSWAP quantum gate. Additionally, the coupling between the NAMR and spins causes a frequency shift on the NAMR that can be detected by a spectrum measurement. This measurement would not affect the states of the spins and could be utilized to prepare entangled states of the spins.

The article is arranged follows: In Sec. II we briefly review the manipulations of a single electronic spin by applying a microwave field, followed by the interaction between the NAMR and one spin. Then, we consider two distant spins simultaneously coupled to an NAMR and discuss how to deliver an effective interaction between the distant spins. Next, we show in Sec. III that the deduced spin-spin interaction can be utilized to implement an iSWAP quantum gate and to generate entangled states of the two spins. Finally, discussions and conclusions are given in Sec. IV.

II. NAMR COUPLES TO DISTANT SPINS

In the setup shown in Fig. 1, two magnetic tips are attached to the end of an NAMR on either side of which two spins are symmetrically placed at a distance h from the NAMR. All the experimental devices are placed in a static magnetic field $\vec{B}_0$ pointing in the positive z-axis direction. Oscillations of the magnetic tips produce a time-varying field, which

*weilianfu@gmail.com

†xbwang@mails.tsinghua.edu.cn

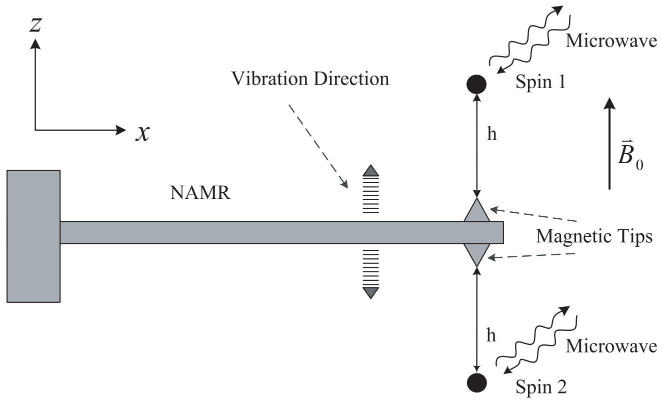

FIG. 1. Sketch for coupling two distant electronic spins via an NAMR. Two magnetic tips are attached to the free end of the NAMR, which mechanically oscillates in the z-axis direction. About 25-nm apart (denoted here by h) from the two tips' equilibrium position there are two electronic spins driven by microwaves.

is proportional to the NAMR's displacement. The NAMR couples with the two spins via the magnetic-field gradient. Microwaves are applied to drive Rabi oscillations between the two states of the spins.

For a single electronic spin driven by microwave field, the Hamiltonian in a frame rotating with the frequency of the microwave field is

$$H_S = -\hbar\delta|\uparrow\rangle\langle\uparrow| + \frac{\hbar\Omega}{2}\left(|\uparrow\rangle\langle\downarrow| + |\downarrow\rangle\langle\uparrow|\right), \tag{1}$$

where Ω denotes Rabi frequency of the transition between the two spin states $|\uparrow\rangle$ and $|\downarrow\rangle$ and δ denotes the detuning between the microwave frequency and the intrinsic frequency of the spin, as shown in Fig. 2(a). The eigenbasis of H_S is given by

$$|g\rangle = \cos(\theta/2)|\uparrow\rangle + \sin(\theta/2)|\downarrow\rangle, \tag{2a}$$

$$|e\rangle = -\sin(\theta/2)|\uparrow\rangle + \cos(\theta/2)|\downarrow\rangle, \tag{2b}$$

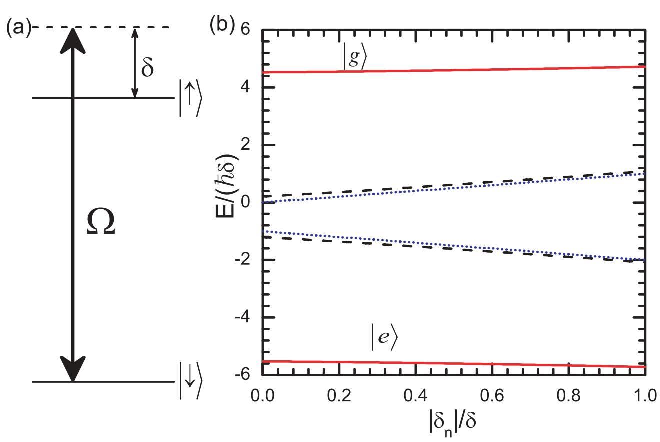

FIG. 2. (Color online) (a) Energy levels for an electronic spin driven by a microwave. (b) Eigenenergies in the presence of hyperfine interactions of the form $H_n = \hbar\delta_n S_z$ caused by the interaction between the nuclear-spin bath magnetic field and the z component of the spin for $\Omega/\delta = 10$ (solid line), $\Omega/\delta = 1$ (dashed line), and $\Omega/\delta = 0.1$ (dotted line).

with $\tan\theta = -\Omega/\delta$. In this basis, the spin can be described by three pseudospin operators: $\sigma_z = |e\rangle\langle e| - |g\rangle\langle g|$, $\sigma_+ = |e\rangle\langle g|$, and $\sigma_- = |g\rangle\langle e|$. The above Hamiltonian can be therefore rewritten as

$$H_S = \tfrac{1}{2}\hbar\omega\sigma_z, \tag{3}$$

with $\omega = (\Omega^2 + \delta^2)^{1/2}$.

Additionally, in this new basis, the z-component of the spin operator $S_z = \frac{\hbar}{2}(|\downarrow\rangle\langle\downarrow| - |\uparrow\rangle\langle\uparrow|)$ reads

$$S_z = \frac{\hbar}{2}[\cos\theta\sigma_z + \sin\theta(\sigma_+ + \sigma_-)]. \tag{4}$$

A. One-spin case

For comparison, we start with the case that the NAMR couples to only one spin. The Hamiltonian of this spin-NAMR system can be written as

$$\hat{H} = H_S + \hbar\omega_r\left(a^\dagger a + \tfrac{1}{2}\right) + \lambda(a^\dagger + a)S_z. \tag{5}$$

The second term describes the quantized vibration of the NAMR with the fundamental frequency ω_r. The last term describes the interaction between the NAMR and the spin with a coupling coefficient $\lambda = g_s\mu_B G_m a_0/\hbar$. Here, μ_B is the Bohr magneton, G_m is the magnetic field gradient, $a_0 = \sqrt{\hbar/(2m_r\omega_r)}$ is the amplitude of zero-point fluctuations for a resonator with effective mass m_r, and $g_s \simeq 2$.

In the interaction picture, Hamiltonian (5) becomes

$$\hat{H}_I = \frac{\hbar\lambda}{2}(e^{-i\omega_r t}a + e^{i\omega_r t}a^\dagger) \times [\cos\theta\sigma_z + \sin\theta(e^{-i\omega t}\sigma_- + e^{i\omega t}\sigma_+)]. \tag{6}$$

Under the usual rotating-wave approximation, Hamiltonian (6) is further simplified to

$$\hat{H}_I(t) \approx \frac{\hbar\lambda_g}{2}(e^{i\Delta t}a^\dagger\sigma_- + e^{-i\Delta t}a\sigma_+) \tag{7}$$

with $\Delta = \omega_r - \omega$ and $\lambda_g = \lambda\sin\theta$.

If the spin and the NAMR work within the so-called large detuning regime wherein $|\lambda_g/\Delta| \ll 1$, then the evolution operator $\hat{U}(t)$ of the system can be well-approximated by

$$\begin{aligned}\hat{U}(t) &= \hat{T}\exp\left[\int_0^t \hat{H}_I(t')dt'\right] \\ &\approx 1 + \left(-\frac{i}{\hbar}\right)^2 \int_0^t \int_0^{t'} \hat{H}_I(t')\hat{H}_I(t'')dt''dt' + \cdots \\ &= \exp\left[-\frac{i}{\hbar}\hat{H}_{\rm eff}t\right],\end{aligned} \tag{8}$$

with the time series operator $\hat{T}$ and the effective Hamiltonian

$$\hat{H}_{\rm eff} = -\frac{\hbar\lambda_g^2}{4\Delta}\left(a^\dagger a + \frac{1}{2}\right)\sigma_z. \tag{9}$$

Returning to the Schrödinger picture, Hamiltonian (9) becomes

$$\begin{aligned}\hat{H} &= \hbar\omega_r'\left(a^\dagger a + \tfrac{1}{2}\right) + \tfrac{1}{2}\hbar\omega\sigma_z \\ &= \hbar\omega_r\left(a^\dagger a + \tfrac{1}{2}\right) + \tfrac{1}{2}\hbar\omega'\sigma_z,\end{aligned} \tag{10}$$

with $\omega_r' = \omega_r - \lambda_g^2\sigma_z/(4\Delta)$ and $\omega' = \omega - \lambda_g^2(a^\dagger a + 1/2)/(2\Delta)$. Obviously, the effective coupling between the spin and NAMR only shifts their eigenfrequencies.

B. Two-spin case

We now consider the generalized two-spin case in which a common NAMR couples simultaneously to two distant spins (see, e.g., Fig. 1). The direct spin-spin interaction can be omitted since it is excessively weak compared with the spin-NAMR interaction [25]. The Hamiltonian of the present system is

$$\tilde{H} = \sum_{i=1,2} H_{Si} + \hbar\omega_r\left(a^\dagger a + \frac{1}{2}\right) + \lambda(a + a^\dagger)(S_{1z} - S_{2z}). \tag{11}$$

Here, the subscript i denotes the spin above or below the NAMR. For simplicity, we set $\omega_1 = \omega_2 = \omega$ by adjusting $\Omega_1 = \Omega_2 = \Omega$ and $\delta_1 = \delta_2 = \delta$ for the two electronic spins. Again, let the system work in the large detuning regime; that is, the NAMR is dispersively coupled to two spins. Then, the effective Hamiltonian of this system is

$$\tilde{H}_{\rm eff} = -\frac{\hbar\lambda_g^2}{4\Delta}\left[\left(a^\dagger a + \frac{1}{2}\right)(\sigma_{1z} + \sigma_{2z}) - (\sigma_{1+}\sigma_{2-} + \sigma_{2+}\sigma_{1-})\right]. \tag{12}$$

This indicates that the vibration mode of the NAMR does not induce the energy exchange between the two electronic spins. It also reveals that quantum nondemolition measurements on the two-spin states could be made by detecting the frequency shift of the NAMR. More importantly, the second term means that the two distant electronic spins can be coupled to each other via the NAMR's quantized motion, which plays the role of data bus. Finally, the induced coupling between the distant spins can be controlled by regulating Δ and λ_g.

Specifically, the present electronic spins could be generated by the N-V centers in diamonds. For realistic situations, we consider the following parameters as an example: $m_r \sim 2.53 \times 10^{-15}$ kg, $h \sim 25$ nm, $G_m = 10^6$ T/m, $a_0 \sim 5 \times 10^{-13}$ m [22], $g_s = 2$, $Q_r = 6 \times 10^5$, and $\omega_r/(2\pi) = 1$ MHz. We choose $\Omega/(2\pi) = 0.9$ MHz and $\delta/(2\pi) = 1$ kHz to satisfy the large detuning and rotating-wave-approximation conditions. The coupling coefficient between the two distant electronic spins is

$$\lambda_e = \frac{\lambda_g^2}{4\Delta} = 3.08 \text{ kHz}. \tag{13}$$

Apparently, this coupling coefficient exceeds the electronic-spin decoherence time (e.g., $T_2 \sim 6$ ms [26]). Also, it should be significantly larger than the damping rate $\kappa \equiv \omega_r/Q_r$ of the NAMR. In fact, the relevant decoherence rate is $\gamma_r \equiv k_B T/(\hbar Q_r)$ for an environment temperature T. Typically, the heating rate is $\gamma_r/(2\pi) = 0.35$ kHz, which is smaller than $\lambda_e/(2\pi)$ for an experimentally accessible temperature $T = 10$ mK. Indeed, for N-V centers, the dephasing time induced by the nuclear-spin fluctuations is observed to be $T_2 = 0.35$ ms [4]. Finally, the nuclear-spin fluctuations may result in vibrations of the spins' upper-energy levels (i.e., the vibrations of δ), which leads to perturbations of ω. We have chosen Ω and δ to satisfy the condition $\delta \ll \Omega$, so the shift of ω_{eg} (i.e., the transition frequency between $|e\rangle$ and $|g\rangle$) caused by these vibrations can be ignored. In Fig. 2(b), we plot the eigenenergies of $H_S' = H_S + H_n(\delta_n)$ as a function of δ_n with $H_n = \hbar\delta_n S_z$. In the eigenbasis of H_S, the perturbations of the ω_{eg} are suppressed for $\Omega \gg |\delta_n|$. Hence, this combination enables us to access the strong-coupling regime of the two spins. Higher values of Q_r or lower temperature T would allow further improvements.

For comparison, we calculate the bare coupling and the maximum-achievable coupling induced by NAMR. Following Takashi [25], the effective coupling strength between two bare spins can be calculated by $J_{\rm eff} = -\mu_0\mu_B^2(\sin^2\theta - 2\cos^2\theta)/[4\pi(2h)^3]$, where μ_0 is the magnetic constant. For the present two distant N-V centers separated by about 50 nm, $J_{\rm eff}/\hbar \sim 0.65$ kHz. Obviously, the induced coupling in Eq. (13) is about 4.7 times larger than the bare coupling. In addition, if $\Delta = 7\lambda_g$ is used as the large-detuning condition by adjusting Ω and δ, then the maximum-achievable coupling is $\lambda_e = (\lambda_g/\Delta)^2\Delta/4 \sim 3.21$ kHz. Certainly, the higher values of ω_r would allow the stronger NAMR-induced coupling.

III. APPLICATIONS

The induced interactions described in the preceding section could be utilized to achieve certain quantum manipulations between the two distant spins, such as for quantum-logic operations and entanglement generations.

A. iSWAP Gate implementation

QIP provides opportunities to tackle problems not feasible with classical methods, such as factoring large prime numbers, searching large unstructured databases, and secure communication. Universal quantum gate is one of the necessary operations for most QIP tasks. As one of the universal quantum gates, iSWAP quantum gates combined with single-bit gates can simulate a unitary operation to arbitrary accuracy. In what follows, we will show how an iSWAP quantum gate can be achieved by using the induced interactions between the two distant spins. The Hamiltonian (12) can be rewritten as

$$\tilde{H}_{\rm eff} = -\frac{\hbar}{4}\left(\frac{\lambda_g^2}{2\Delta}\right)\left[2\left(a^\dagger a + \frac{1}{2}\right)(\sigma_{1z} + \sigma_{2z}) - (\sigma_{1x}\otimes\sigma_{2x} + \sigma_{1y}\otimes\sigma_{2y})\right], \tag{14}$$

which means that the evolution operator of the system after the time $t = 6\pi\Delta/\lambda_g^2$ is given by

$$\tilde{U}_S = \exp\left[-i\frac{\tilde{H}_{\rm eff}}{\hbar}t\right] = \begin{pmatrix} e^{i\varphi} & 0 & 0 & 0 \\ 0 & 0 & i & 0 \\ 0 & i & 0 & 0 \\ 0 & 0 & 0 & e^{-i\varphi} \end{pmatrix}, \tag{15}$$

where $\varphi = 3\pi(n + 1/2)$ with $n = \langle a^\dagger a\rangle$ being the average phonon number in the NAMR. Compared with the matrix form of an iSWAP quantum gate, an unwanted global phase φ is introduced. Fortunately, this global phase can be eliminated by the single qubit phase rotations $|0\rangle \rightarrow e^{i\varphi/2}|0\rangle$ and $|1\rangle \rightarrow e^{-i\varphi/2}|1\rangle$ if n is known in advance.

B. Entanglement preparation

Returning to the Schrödinger picture, Hamiltonian (12) is given by

$$\tilde{H} = H_S'' + \hbar\omega_r'\left(a^\dagger a + \tfrac{1}{2}\right), \tag{16}$$

where $H_S'' = \hbar\omega(\sigma_{1z}+\sigma_{2z})/2 + \hbar\lambda_g^2(\sigma_{1+}\sigma_{2-}+\sigma_{1-}\sigma_{2+})/(4\Delta)$ is the Hamiltonian associated with only the two spins and $\omega_r' = \omega_r + \delta\omega_r$ with

$$\delta\omega_r = -\frac{\lambda_g^2}{4\Delta}(\sigma_{1z}+\sigma_{2z}). \tag{17}$$

Equation (17) shows that the frequency shift depends on the eigenvalues of σ_{1z} and σ_{2z}. Compared with the spectrum of the NAMR without spins, the two spins in the same state shift the positions of the spectral peaks due to the quantum motion of the NAMR, which is larger than the classical-NAMR case [27]. When the two electronic spins are in $|e_1g_2\rangle$ or $|g_1e_2\rangle$, the coefficient $(\sigma_{1z}+\sigma_{2z})$ of Eq. (17) is zero and would result in no frequency shift.

To show that the frequency shift is large enough to be distinguished in the presence of the environmental noise and can be measured within the decoherence time of the spin, we now study the frequency spectrum of the NAMR's position, including the effect of the fluctuation-dissipation processes which would disturb the dynamics of the NAMR by affecting the mechanical mode. In the presence of dissipation, the motion equations of the NAMR can be deduced from the quantum Langevin equations:

$$\dot{z}(t) = \frac{p(t)}{m_r}, \tag{18a}$$

$$\dot{p}(t) = -m_r\omega_r'^2 z(t) - \gamma\dot{z}(t) + \xi(t), \tag{18b}$$

where $z(t)$ and $p(t)$ are the position and corresponding momentum operators of the NAMR, respectively. The mechanical mode is affected by a viscous force with damping rate γ and a Brownian stochastic force with zero mean value $\xi(t)$ with the mean anticommutator [28]

$$\langle[\xi(t),\xi(t')]_+\rangle = \frac{\gamma\hbar}{\pi}\int_{-\infty}^{+\infty} d\omega e^{-i\omega(t-t')}\omega\coth\left(\frac{\hbar\omega}{2k_BT}\right), \tag{19}$$

where k_B is the Boltzmann constant. By performing a Fourier transform of $z(t)$ and solving equations (18a) and (18b), we have the NAMR spectrum

$$S_z(\omega) = \frac{S_\xi(\omega)}{m_r^2\left(\omega^2-\omega_r'^2\right)^2 + \omega^2 S_R(\omega)}, \tag{20}$$

where $S_\xi(\omega)$ and $S_R(\omega)$ are the spectra due to the reservoir and the viscous force, respectively.

Consider the NAMR with the parameters given above as an example. Under the first Markov approximation, $S_R(\omega) = |\gamma|^2$ and $S_\xi(\omega) = \frac{\hbar\omega\gamma}{2\pi}\coth(\frac{\hbar\omega}{2k_BT})$ with $\gamma = 4\pi m_r\omega_r/Q_r$. For a temperature of $T = 10$ mK, the frequency shift is about 0.98 kHz with a full width at half maximum (FWHM) of about 21 Hz, as shown in Fig. 3(a). The three curves can be distinguished. The spectrum measurement can be completed in microseconds, which is within the spin's decoherence time. Thus, this frequency shift is detectable.

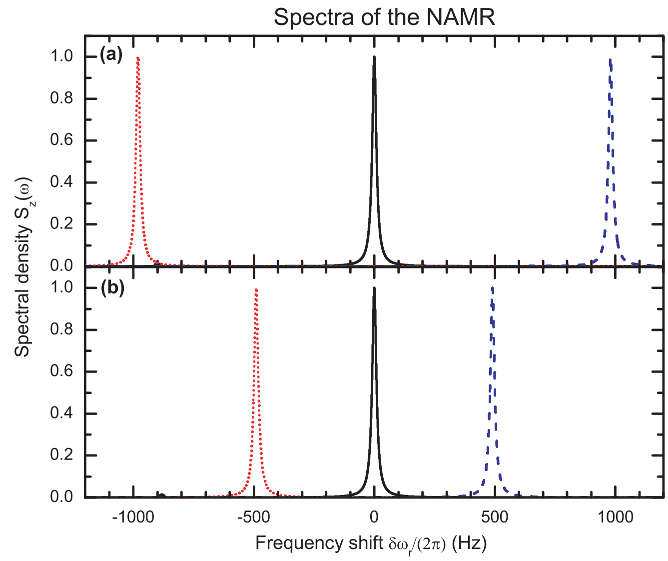

FIG. 3. (Color online) (a) Frequency shift for the two-spin case. The black (or solid) curve denotes no frequency shift when the two electrons are in $|e_1g_2\rangle$ or $|g_1e_2\rangle$. The red (or dotted) curve and blue (or dashed) curve denote a frequency shift of about 980 Hz when the two electrons are in $|e_1e_2\rangle$ and $|g_1g_2\rangle$, respectively. (b) Frequency shift for the one spin case. The solid curve is the spectrum without spin.

For the one-spin case, the frequency shift is shown in Fig. 3(b), which is almost half of the two-spin case. In this case, the interaction between NAMR and one spin always results in a frequency shift. Whereas for the two-spin case, if the two spins are in opposite states in the eigenbasis, zero frequency shift occurs for the NAMR. As a consequence, entangled states of the two spins could be produced by detecting the frequency shift of the NAMR without affecting the states of the spins. For example, if the spins and NAMR are prepared in the initial state $|\uparrow\uparrow\rangle \otimes |n\rangle$ then, at time t afterward, the state of this system reads

$$|\chi_{SN}\rangle = \left\{\sin^2(\theta/2)e^{i\lambda_e bt}|ee\rangle + \cos^2(\theta/2)e^{-i\lambda_e bt}|gg\rangle - \frac{1}{\sqrt{2}}\sin\theta e^{-i\lambda_e t}\left[\frac{1}{\sqrt{2}}(|eg\rangle+|ge\rangle)\right]\right\}\otimes|n\rangle, \tag{21}$$

with $b = 2a^\dagger a + 1$. When zero frequency shift is detected, the maximal entangled state

$$|\chi_f\rangle = \frac{1}{\sqrt{2}}(|eg\rangle + |ge\rangle) \tag{22}$$

of the two spins could be produced with a success probability proportional to $\sin^2\theta$. Here, we have neglected the insignificant global phase factor $-e^{-i\lambda_e t}$. Certainly, if the measurement result gives a frequency shift, no entangled state can be obtained.

IV. DISCUSSIONS AND CONCLUSION

Perfect accuracy is impossible in practical experiments, so we now discuss the imperfect situation; namely that the symmetry of the spins' placements is slightly broken. The two tips on the free end of the NAMR can be treated as a magnetic dipole and produce a field $B_{\mathrm{tip}} = B_{z0} + G_{\mathrm{m}} z$. Here, B_{z0} is a constant field which is independent of z, $G_{\mathrm{m}} = h^{-4}(A_{\mathrm{m}} + B_{\mathrm{m}} h^{-2}\rho^2)$ is the field gradient with ρ being the distance between the spins and the z axis, and A_{m} and B_{m} are the two constants determined by the magnetic-dipole moments. The asymmetric positions of the two spins have different magnetic gradients, which would lead to different coupling coefficients between the spins and the NAMR. As a consequence of this asymmetry, the terms $\lambda_g^2(\sigma_{1z} + \sigma_{2z})$ and $\lambda_g^2(\sigma_{1+}\sigma_{2-} + \sigma_{2+}\sigma_{1-})$ in the effective Hamiltonian (12) are replaced by new terms $(\lambda_{g1}^2\sigma_{1z} + \lambda_{g2}^2\sigma_{2z})$ and $\lambda_{g1}\lambda_{g2}(\sigma_{1+}\sigma_{2-} + \sigma_{2+}\sigma_{1-})$. The magnitude of the NAMR frequency shift is replaced by $(\lambda_{g1}^2 + \lambda_{g2}^2)/2$ instead of λ_g^2, and a small frequency shift of the order of $|\lambda_{g1}^2 - \lambda_{g2}^2|/2$ occurs, compared with the symmetry condition.

In conclusion, two distant spins can be strongly coupled together via the quantized motion of an NAMR. In the large-detuning regime, the motion of the NAMR does not excite transitions between the spin's states. In the one-spin case, the effective interaction between the spin and the NAMR only shifts their intrinsic frequency and transition frequency. In the two-spin case, an effective interaction term between the two distant spins occurs. The strong-coupling regime can be still accessed in the presence of fast dephasing of the spins because of interactions with the nuclear bath. More importantly, this coupling can be controlled by adjusting the microwave frequency and the detuning. Meanwhile, the spectrum measurement of the NAMR does not affect the states of the spins. The two spins in different states may cause zero frequency shift of the NAMR. Thus, the maximal entangled states of the two spins can be probabilistically generated by detecting the frequency shift of the NAMR.

ACKNOWLEDGMENTS

This work is partially supported by the NSFC Grants No. 10775091, No. 10874142, No. 60725416, and No. 90921010, China Hi-Tech program Grant No. 2006AA01Z420, and by the National Fundamental Research Program of China through Grants No. 2007CB807900, No. 2007CB807901, and No. 2010CB923104.

[1] J. Wrachtrup and F. Jelezko, J. Phys. Condens. Matter **18**, S807 (2006).
[2] M. A. Nielsen and I. L. Chuang, *Quantum Computation and Quantum Information* (Cambridge University Press, Cambridge, 2000).
[3] Charles H. Bennett and P. DiVincenze, Nature (London) **404**, 247 (2000).
[4] Torsten Gaebel *et al.*, Nat. Phys. **2**, 408 (2006).
[5] K. L. Ekinci and M. L. Roukes, Rev. Sci. Instrum. **76**, 061101 (2005).
[6] Scott S. Verbridge, Harold G. Craighead, and Jeevak M. Parpia, Appl. Phys. Lett. **92**, 013112 (2008).
[7] I. De Vlaminck *et al.*, Appl. Phys. Lett. **90**, 233116 (2007).
[8] M. D. LaHaye *et al.*, Science **304**, 74 (2004).
[9] N. O. Azak *et al.*, Appl. Phys. Lett. **91**, 093112 (2007).
[10] T. Kouh *et al.*, Appl. Phys. Lett. **86**, 013106 (2005).
[11] K. L. Ekinci, X. M. H. Huang, and M. L. Roukes, Appl. Phys. Lett. **84**, 4469 (2004).
[12] B. Ilica and H. G. Craighead, J. Appl. Phys. **95**, 3694 (2004).
[13] A. Naik, O. Buu, M. D. LaHaye, and D. Rugar, Nature (London) **443**, 193 (2006).
[14] Dustin Kleckner and Dirk Bouwmeester, Nature (London) **444**, 75 (2006).
[15] M. Poggio *et al.*, Phys. Rev. Lett. **99**, 017201 (2007).
[16] L. Tian, Phys. Rev. B **72**, 195411 (2005).
[17] Xingxiang Zhou and Ari Mizel, Phys. Rev. Lett. **97**, 267201 (2006).
[18] Fei Xue, Yu-xi Liu, C. P. Sun, and F. Nori, Phys. Rev. B **76**, 064305 (2007).
[19] M. P. Blencowe and E. Buks, Phys. Rev. B **76**, 014511 (2007).
[20] Lieven M. K. Vandersypen, Nature Phys. **3**, 83 (2007).
[21] D. Rugar *et al.*, Nature (London) **430**, 329 (2004).
[22] P. Rabl, P. Cappellaro, M. V. Gurudev Dutt, L. Jiang, J. R. Maze, and M. D. Lukin, Phys. Rev. B **79**, 041302(R) (2009).
[23] P. Rabl *et al.*, e-print arXiv:0908.0316.
[24] Z. Y. Xu, Y. M. Hu, W. L. Yang, M. Feng, and J. F. Du, Phys. Rev. A **80**, 022335 (2009).
[25] Takashi Itoh, Rev. Mod. Phys. **37**, 159 (1965).
[26] P. Neumann *et al.*, Science **320**, 1326 (2008).
[27] L. F. Wei, Y. X. Liu, C. P. Sun, and F. Nori, Phys. Rev. Lett. **97**, 237201 (2006).
[28] C. W. Gardiner and P. Zoller, *Quantum Noise*, 3rd ed. (Springer, New York, 2004).